Twin Telescope Tests: Assessing Station Oriented Systematic Errors

C. S. Jacobs, C. García-Míro, S. Horiuchi, L.G. Snedeker

Abstract Each of NASA's three Deep Space Network sites has multiple large antennas capable of acquiring VLBI data. The long range plan is to have four 34-meter beam waveguide antennas at each site. At present Goldstone has three, Canberra has three, and Madrid has two with two more under construction. These antennas offer the opportunity to do connected element interferometry (CEI) over the few hundred meter baselines within each complex. Given that all antennas within a site are of nominally the same structural design, are run off the same clock, observe through almost the same atmosphere, and are subject to almost the same geophysics, doing CEI experiments is an excellent way to probe the limits of VLBI accuracy and expose station-specific systematic errors. This paper will report the results of just such tests which achieved about 0.2 mm baseline precision per pass. Some stations exhibit more than 1 mm systematics. Based on this data we will discuss the implications for whether the IAG's goal of 1 mm station stability in VLBI geodesy is possible for large antennas.

Keywords VLBI, reference frame, ITRF, quasar, AGN, station stability

Christopher Jacobs
JPL, California Institute of Technology/NASA, Pasadena, CA
Cristina García Míro
Madrid Deep Space Communications Complex/NASA, ISDEFE, Madrid, Spain
Shinji Horiuchi
Canberra Deep Space Communications Complex/NASA, CSIRO, Canberra, Australia
Larry Snedeker
Goldstone Deep Space Communications Complex/NASA, SaiTech, Ft. Irwin, CA

1 Introduction

Modern geodetic techniques have an important role to play in many aspects of society. Driven by concerns about global sea level rise, the International Association of Geodesy (IAG) has set requirements for the next generation International Terrestrial Reference Frame (ITRF) to have an accuracy of ± 1 mm in global positioning (e.g. Beutler, et al (2009)). Current Very Long Baseline Interferometry (VLBI) measurements have errors much larger than this ± 1 mm goal. Tropospheric fluctuations in refractivity, largely from water vapor (e.g. Treuhaft & Lanyi (1987)), stochastic variations in station clocks, and extended source morphology (e.g. Charlot (1990)) are commonly cited as the major sources of error in VLBI. Are these the only error sources larger than 1 mm?

This paper leverages a short baseline (200–300 m) configuration so that most of the tropospheric, clock, (global) geophysical, and source structure errors common mode away thereby revealing underlying instrumental errors. Furthermore, because the experiments discussed here used antennas of nominally the same design, structural deformation due to gravity loading should largely common mode. Thermal expansion should common mode to the extent that both antennas are in the same thermal environment. Note that our previous work (Jacobs & Rius (1989)) using antennas of radically different sizes and designs i.e. the 70-m (DSS 63) and the old non-beam waveguide 34-m (DSS 65) could not leverage common mode-ing of structural errors to anywhere near the $\pm$ 1mm accuracy goal of the current work.

Geophysical motion should common mode away to the extent that both antennas are attached to the same piece of stable bedrock. In summary, these experiments have the potential to be a null test to verify the preceding assumptions that most error sources common mode away down to the accuracy goal level of ± 1 mm. Our experience at NASA's Goldstone site circa 2005 accomplished just such verification. However, the data from our Madrid site indicated that not all antennas performed at the ± 1 mm accuracy level.

2 Observations and Data Analysis

As shown in Table 1, a series of short baseline Connected Element Interferometry (CEI) passes were done between 2014 and 2017 at the Canberra and Madrid Deep Space Network (DSN) sites. The CEI technique we used is virtually the same as VLBI except that, unlike VLBI, both stations were synchronized to the same H_2 maser clock thereby virtually eliminating clock variations as an error source—other than minor differences in clock distribution to the two antennas.

The observation schedules were designed to sample the full range of azimuth, cable wrap, and elevation using the strong ICRF2 defining sources (Ma et al (2009)) which have sufficiently accurate astrometric positions to be fixed a priori for the short $\sim$200 m baselines under consideration. Sky coverage was optimized within the constraint of keeping slew times manageable by nodding up and down in elevation while rotating in azimuth in steps on the order of 20°. The schedule moved through the full range of cable wrap including the full 360° of azimuth plus reaching a full quadrant from both clockwise and counterclockwise directions. This schedule strategy separates geometric baseline effects due to azimuth changes from cable wrap effects. Sessions were typically 4–8 hours and done at night when possible to minimize thermal gradients.

We used the DSN 34-meter beam waveguide (Imbriale (2002)) antennas to observe X-band (8200–8600 MHz) with Right Circular Polarization. The data were downconverted by subtracting 8100 MHz, sent over cables to the control room where the analog signal was digitized by the Wideband VLBI Science Recorder (Rogstad et al. (2009)) with 2-bit resolution, and channelized into 12 channels each 8 MHz wide for a total data rate of 384 Mbps per station. The data were e-transferred to JPL, correlated with the SOFTC software correlator (Lowe (2006)), and fringe fit with the CFit software to produce group delays and phase delay rates. These observables were then modelled using the MODEST software (Sovers et al. (1998)). We estimated parameters for a differential baseline vector, differential zenith troposphere, and differential time-linear residual clock.

Date	stations	Scans	wRMS (psec)
	Canberra		
2014 05 28	DSS 34–35	317	4.6
2014 07 12	DSS 34–35	132	6.3
2014 07 19	DSS 34–35	153	2.7
2014 07 25	DSS 34–35	261	11.2
2016 06 18	DSS 34–35	178	4.4
2016 07 14	DSS 34–36	111	3.7
2016 07 17	DSS 34–36	125	11.4
2016 09 23	DSS 34–36	188	3.3
	Madrid		
2015 12 05	DSS 54–55	119	5.2
2016 01 31	DSS 54–55	132	5.4
2016 05 07	DSS 54–55	167	4.1
2016 07 09	DSS 54–55	93	5.2
2017 01 03	DSS 54–55	188	3.3

Table 1 Summary of Observations. All sessions used X-band RCP recorded at 384 Mbps.

3 Delay Scatter Results

Table 1 shows the dates, the pair of Deep Space Stations (DSS), the number of scans and the wRMS group delay scatter. Most passes show a scatter of 3–6 psec or 1–2 mm. There are two passes close to 4 mm scatter. As an example, Fig. 1 shows the group delay vs. time on 2014 May 28 on the DSS 34 to DSS 35 baseline. The 4.5 psec scatter is equivalent to about 1.4 mm. The points with orange color coding are close to the sun suggesting that thermal effects may be increasing the delay scatter at the start of the pass.

4 Case Study: Madrid Systematic Error Level

The Madrid complex is shown in Fig 2. Within this complex, the DSS 54 to DSS 55 baseline was measured five times between 2015 Dec. and 2017 Jan. Fig. 3 shows the baseline length scatter is extremely stable

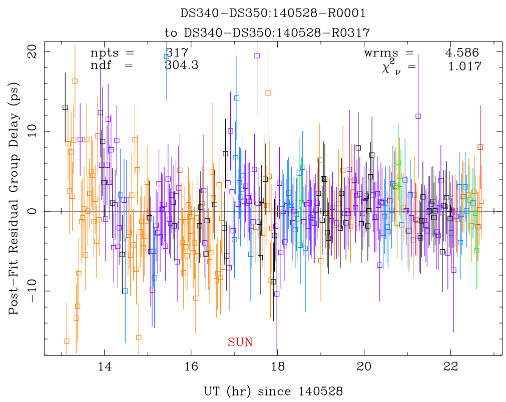

Fig. 1 Group delay scatter on Australia's DSS 34 to DSS 35 baseline on 2014 May 28. Orange indicates scans near the Sun.

with a wRMS scatter of 0.11 mm. Fig. 4 shows the vertical scatter is 0.26 mm excepting the outlier session on 2016 Jul 09 which had a sunrise in the middle. Thus the length and vertical results confirm our expectation that errors should common mode away down to the 1 mm level. However, the horizontal baseline history raised questions. Both the East (Fig. 5) and North (Fig. 6) components showed a monotonic, roughly linear increase for the first four sessions at the level of ≈ 3 mm/yr. By the time the 4^{th} session's results were analyzed, we were becoming increasingly concerned that there was a differential velocity between DSS 54 and DSS 55 which might eventually damage an antenna. Thus we began to focus on the foundations.

5 Antenna Foundation

Foundations are critical to the stability of the antenna's position and thus the intra-complex baseline vectors that we are measuring. Our starting assumption is that all antennas within a given complex are firmly attached to the same piece of bedrock thereby eliminating any geophysically induced differential motion from slippage or seasonal variation in underlying groundwater. Fig. 7 shows the foundation work for the under-construction DSS 56 antenna as of 2016 Nov 10. This photograph reveals the sub-surface geology within a few 100 m of the antennas we measured (DSS 54 and 55). The surface soil extends 0–10 m after which one observes a mixture of soil and rock. To the left, the terrain is almost bedrock, but has an underlying thin seam of soil which might allow seismic movement or ground water induced changes. The construction seeks to get below these seams to solid bedrock before laying the concrete foundation shown in Fig. 7.

This quick lesson in foundations failed to reveal why the east and north were not stable. And, in fact, when the results of the 5th and final session were analyzed, both the east and north values came down thereby breaking the linear trend. We note that a 6th session done after these results were presented also went against the linear trend and began to suggest that we are seeing a seasonal effect of unknown origin. We have begun to consider a range of effects such as differential thermal environment due to the downward topography going from DSS 54 to DSS 55 (Fig. 2) or phase and delay effects from antenna pointing errors (Gorham & Rochblatt (1998)) or—returning to foundations—local hydrological effects such as groundwater getting under one of the foundations.

6 Conclusions

The goal of the twin telescope baseline measurements discussed in this paper has been to measure the baseline in an environment in which most error sources difference away so that variations in individual antennas can be isolated and studied. We have presented a series of short baseline Connected Element Interferometry (CEI) sessions from NASA's Deep Space Network complexes with eight passes from Canberra, Australia and five passes from Madrid, Spain. These passes had 1 to 4 mm of group delay scatter per session. The Canberra, Australia baselines were generally stable to near the ± 1 mm level.

The early Madrid measurements showed a trend of a few mm/yr in the horizontal components. Only later did it appear that the 2016 Jul 09 session was an outlier—not only the obvious vertical but also the horizontal components. Removing that outlier session, wRMS scatters become 0.29 mm in east, 0.18 mm in north, 0.22 mm in vertical, and 0.08 mm in length.

Our previous experience, especially at the Goldstone complex, has been that the vertical component has a factor of several higher scatter than the horizontal components. This is expected because (1) vertical is

Fig. 2 Aerial view of NASA's Madrid Deep Space Communications Complex. There are three active 34-m antennas (DSS 54, 55, and 65), a 70-m (DSS 63), an inactive 34-m antenna (DSS 61), and two 34-m antennas under construction (DSS 53 & 56). The four antennas DSS 53, 54, 55, and 56 are all nominally of the same beam waveguide design (Imbriale (2002)).

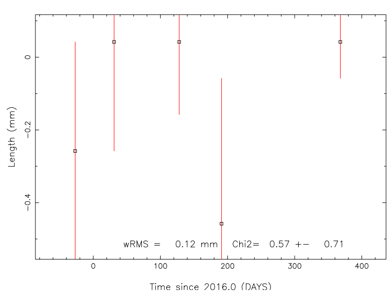

Fig. 3 Length vs. time, DSS 54−55. wRMS = 0.12 mm

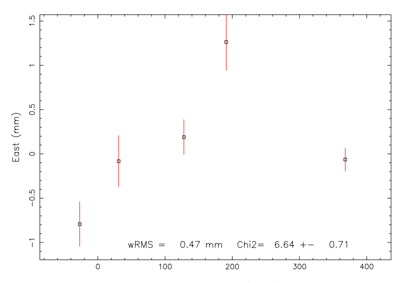

Fig. 5 East vs. time for DSS 54−55. wRMS = 0.47 mm

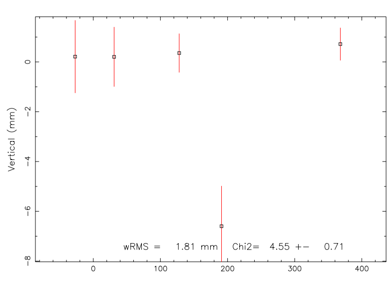

Fig. 4 Vertical vs. time, DSS 54−55. wRMS = 1.81 mm

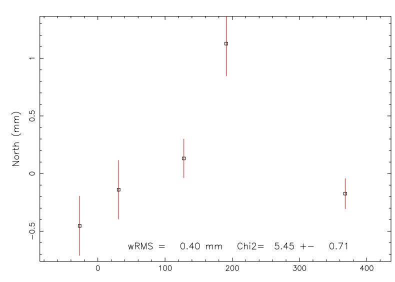

Fig. 6 North vs. time for DSS 54−55. wRMS = 0.40 mm

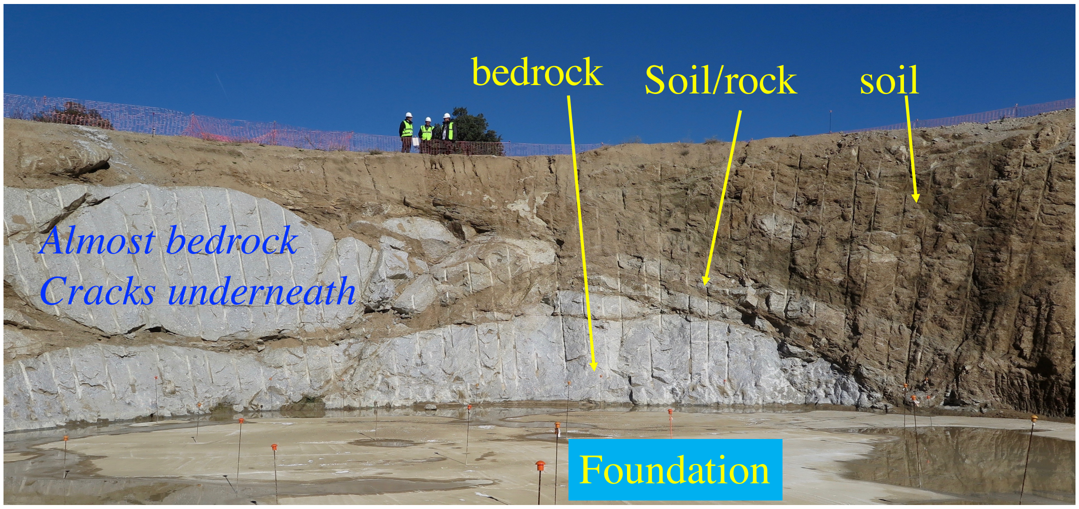

Fig. 7 Progress as of 2016 Nov. 10th on the construction of the foundation for a new 34-meter beam waveguide antenna, Deep Space Station (DSS) 56. Foundations are intended to be attached to solid bedrock to provide stable baselines throughout the complex.

determined from $< 90^\circ$ of elevation range vs. the horizontal's 360° range of observations and (2) troposphere degrades the vertical more than horizontal.

Efforts to understand these results are ongoing. At this time, the small sample size makes it difficult to establish an outlier with certainty. Our plan is to make measurements of the DSS 54 to DSS 55 baseline at roughly quarterly intervals with the hope that outliers and seasonal effects can be well separated as a step towards understanding the error budget in this class of measurements. Once we understand the instrumental and possible local geophysical and hydrological effects on these short intra-complex baselines to the 1 mm level, we will have achieved a small but important step towards the goal of global geodesy at the 1 mm level.

Acknowledgements

 U.S. Government sponsorship acknowledged for the work done at JPL-Caltech under a contract with NASA. Thanks to Hana Krásná and Marisa Nickola for comments which improved this paper and to María Benítez-Balseiro for the tour of the DSS 53 and DSS 56 foundations.

References

P. Charlot, 'Radio-source Structure in Astrometric and Geodetic VLBI,' *AJ*, 99, pp. 1309–1326, 1990.

G. Beutler, M. Pearlman, H.-P. Plag, R. Neilan, M. Rothacher, R. Rummel, 'Global Geodetic Observing System - Meeting the Requirements of a Global Society on a Changing Planet in 2020,' *in* Towards GGOS in 2020, Springer, H.-P. Plag, M. Pearlman, eds., pp. 273–281, chapter 10, 2009.

P.W. Gorham & D.J. Rochblatt, 'Effect of Antenna-Pointing Errors on Phase and Interferometric Delay,' *JPL TDA Prog. Report*, 42-132, 15 Feb. 1998.

W.A. Imbriale, 'Large Antennas of the Deep Space Network,' chapter 8: The 34-Meter Beam-Waveguide Operational Antennas,' *Deep Space Communications and Navigation Series*, DESCANSO Monograph 4, J. Yuen, ed., chapter 8, pp. 225–255, 2002.

C.S. Jacobs & A. Rius, 'VLBI Surveying between DSS63 and DSS65,' *Proc. 7th EVGA*, p. 64–67, 1989.

S.T. Lowe, 'SOFTC: A Software Correlator for VLBI,' *NASA Technical Report Server*, NASA Tech Briefs, p. 43, 2006.

C. Ma, et al, 'The Second Realization of the International Celestial Reference Frame by VLBI,' A. Fey, D. Gordon, & C.S. Jacobs, eds., *IERS Tech Note No. 35*, BKG, 2009.

S. Rogstad, R. Navarro, S. Finley, C. Goodhart, R. Proctor, and S. Asmar, 'The Portable Radio Science Receiver (RSR),' *JPL IPN Progress Report*, 42-178, 2009.

O.J. Sovers, J.L. Fanselow, and C.S. Jacobs, 'Astrometry and Geodesy with Radio Interferometry: Experiments, Models, Results,' *Rev. Mod. Phys.*, 70, 4, 1998.

R.N. Truehaft & G.E. Lanyi, 'The Effect of the Dynamic Wet Troposphere on Radio Interferometric Measurements,' *Radio Sci.*, 22, pp. 251–265,1987.